Dynamic Analysis of a Three-Degrees-of-Freedom In-Parallel Actuated Manipulator

KOK-MENG LEE AND DHARMAN K. SHAH

Abstract—**Despite the voluminous publications on robot dynamics and control, the literature to date is based solely on the serial link manipulators. Little attention has been given to the alternative manipulator design based on the concept of in-parallel actuated mechanism, which is characterized by its excellent rigidity, high strength-to-moving-weight ratio, and relatively simple inverse kinematics. This communication presents the dynamic analysis of a three-degrees-of-freedom in-parallel actuated manipulator. The equations of motion have been formulated in joint space using Lagrangian approach. The analysis provides the solution to predict the forces required to actuate the links so that the manipulator follows a predetermined trajectory. A dynamic simulation program which has been developed illustrates the influence of the link dynamics on the actuating force required. The dynamic analysis provides a basis for future theoretical research to develop the control scheme, for experimental research to estimate the inertia parameters, and for design optimization of the prototype manipulator.**

I. Introduction

Recently, some effort has been directed towards alternative manipulator designs based on the concepts of closed kinematic chain mechanism to improve manipulator rigidity and strength-to-weight ratio. The closed kinematic chain mechanism, in general, has relatively simple inverse kinematics as compared to the conventional open kinematic chain mechanism. The closed kinematic chain manipulator has potential applications where the demand on workspace and maneuverability is low but the dynamic loading is severe and high speed and precision motion are of primary concern.

Typical examples of in-parallel mechanism are the camera tripod and the six-degrees-of-freedom Stewart platform. The Stewart platform was originally designed as an aircraft simulator [1], later as a robot wrist [2], and as a tendon actuated in-parallel manipulator [3], [4]. Various applications of the Stewart platform were investigated for use in mechanized assembly [5] and as a compliance device [6]. The kinematics and practical design considerations of the Stewart platform for use as a manipulator were considered in [7], [8]. A systematic review on possible alternative in-parallel mechanisms and other combinations in which part of the manipulator is serial and part parallel were addressed in [9], [10]. Recently, some efforts were directed towards the dynamic analysis of the Stewart platform using the Newton–Euler method [11] and screw theory [12]. A more general analysis for the six-degree-of-freedom (DOF) multiloop parallel manipulators was discussed in [13] and [14].

Apart from the Stewart platform manipulator, Landsberger and his co-workers at MIT [4] have constructed a 3-DOF in-parallel tendon-actuated positioner as a first step to Stewart platform implementation. Since the tendon is essentially massless and the spine of the 3-DOF positioner is hydraulically driven, the positioner dynamics are primarily due to the hydraulic servo and the unknown payload. Although no analytical dynamic simulation result was presented, experimental simulation was made to prove the concept feasibility. The 3-DOF positioner has the advantages of being lightweight, simple dynamics and control, and is well-suited for tasks (such as lifting objects or welding) where the demands on compression load are of less concern as compared to that on tension load through the tendons.

Small working space is commonly recognized as one of the drawbacks of the Stewart platform manipulator as compared to a serial link manipulator. The authors have performed the kinematic analysis of a 3-DOF tripod-like manipulator which has two orientation freedoms and one translatory freedom based on the concept of in-parallel actuated mechanism [15], [16]. In particular, the closed-form solution of the inverse kinematics were presented and the influences of physical constraints on the range of motion were discussed in [15]. Also, various potential applications where the 3-DOF in-parallel actuated manipulator may be used as part of the 6-DOF manipulator system to enlarge the working space were highlighted in [15] and [17].

This communication focuses on the dynamic analysis of a 3-DOF in-parallel manipulator using Lagrangian approach. In particular, the communication presents the formulation of the dynamic equations in joint space and the solutions which determine the forces/torques required to follow a prescribed trajectory. An example of tracing a helical path is chosen to illustrate the dynamic simulation and to show that the Cartesian position of the moving platform may be controlled at a sacrifice of orientation freedoms. In applications such as unattended precision machining and fixturing, where both high dynamic compression and tension loading are required, the tendon-driven in-parallel actuated manipulator is less rigid than optimum. Hence, the influences of link dynamics are highlighted by means of dynamic simulation results.

II. Kinematics

A schematics of the 3-DOF in-parallel actuated manipulator is shown in Fig. 1. The manipulator consists of a base platform, three extensible links, and a moving platform which houses the driving mechanism of the gripper. The moving platform is connected to the links by means of ball joints which are equally spaced at 120° and at a radius r from the center of the moving platform. The other ends of the links are connected to the base platform through equally spaced pin joints at a radius R from the center of the base platform. By varying the link lengths, the moving platform can be manipulated with respect to the base platform.

As shown in Fig. 1, a base coordinte frame which is designated as XYZ frame is fixed at the center of the base platform with its Z-axis pointing vertically upward and the X-axis pointing towards the pin joint 1, $P1$. Similarly, a coordinate frame xyz is assigned to the center of the upper platform, with the z-axis normal to the platform and the x-axis pointing towards the ball joint 1, $b1$. The coordinate frame xyz with respect to the base coordinate frame XYZ can be described by the homogeneous transformation $[T]$

$$[T]=\begin{bmatrix} n_1 & o_1 & a_1 & x_c \\ n_2 & o_2 & a_2 & y_c \\ n_3 & o_3 & a_3 & z_c \\ 0 & 0 & 0 & 1 \end{bmatrix} \tag{1}$$

where $(x_c, y_c, z_c)^T$ describes the position of the origin of the xyz frame and the orientation vectors $(n_1, n_2, n_3)^T$, $(o_1, o_2, o_3)^T$, and $(a_1, a_2, a_3)^T$ are the directional cosines of the axes x, y, and z with respect to the base frame XYZ.

In the dynamic analysis of the manipulator, both the inverse and forward kinematics are necessary. As the derivation of the kinematic equations has been discussed in [15], only the result of kinematic analysis are presented here.

A. Inverse Kinematics

In terms of Z–Y–Z Euler angles, it has been determined in [15] that the two orientation freedoms of the moving platform with respect to the base platform are the precession angle α and the nutation angle

Manuscript received November 3, 1986; revised October 21, 1987. This work was supported by the Georgia Institute of Technology under the general research fund and by the Computer Integrated Manufacturing Systems (CIMS) Program.

The authors are with The George Woodruff School of Mechanical Engineering, Georgia Institute of Technology, Atlanta, GA 30332.

IEEE Log Number 8718915.

0882-4967/88/0600-0361$01.00 © 1988 IEEE

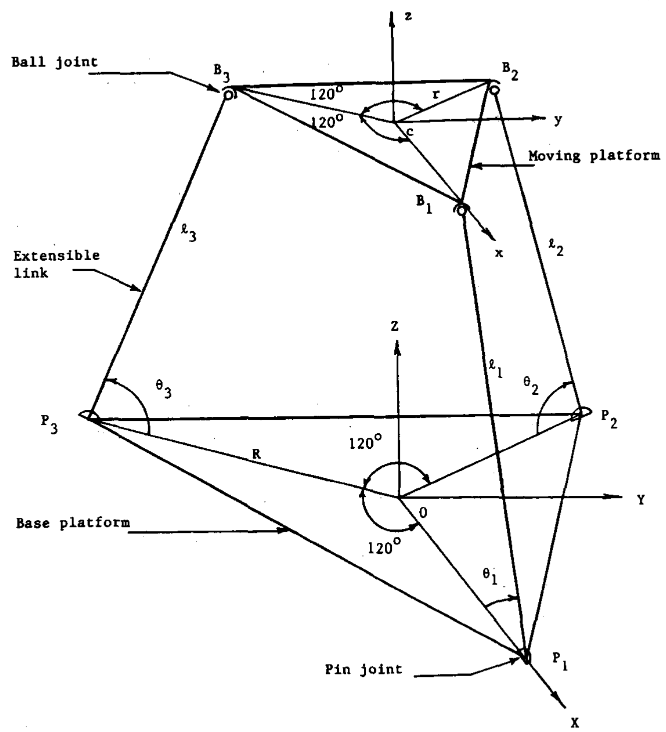

Fig. 1. Three-degree-of-freedom in-parallel actuated mechanism schematic.

β. The Cartesian translatory freedom is in the Z direction. The spin angle of the moving platform γ, with respect to the base platform, has been determined to be

$$\alpha = -\gamma \tag{2}$$

and the other two Cartesian position variables in the X and Y directions are

$$X_c = -\frac{1}{2}\rho(1-C_\beta)C_{2\alpha} \tag{3}$$

$$Y_c = \frac{1}{2}\rho(1-C_\beta)S_{2\alpha} \tag{4}$$

where $C_\beta = \cos\beta$, $S_{2\alpha} = \sin 2\alpha$, $C_{2\alpha} = \cos 2\alpha$, $\rho = r/R$, $X_c = x_c/R$, and $Y_c = y_c/R$. The actuating lengths of the links for a prescribed position and orientation of the moving platform have been expressed in terms of Z-Y-Z Euler angle as

$$L_1^2 = 1+\rho^2+X_c^2+Y_c^2+Z_c^2-2X_c+2\rho(C_\alpha^2C_\beta+S_\alpha^2)(X_c-1) + \rho(C_\beta-1)S_{2\alpha}Y_c-2\rho S_\beta C_\alpha Z_c \tag{5}$$

$$\begin{aligned} L_2^2 = {} & 1+\rho^2+X_c^2+Y_c^2+Z_c^2+X_c-\sqrt{3}\,Y_c \\ & -\rho[C_\alpha^2C_\beta+S_\alpha^2-\sqrt{3}\,C_\alpha S_\alpha(C_\beta-1)]\left[X_c+\frac{1}{2}\right] \\ & -\rho[S_\alpha C_\alpha(C_\beta-1)-\sqrt{3}(S_\alpha^2C_\beta+C_\alpha^2)]\left[Y_c-\frac{\sqrt{3}}{2}\right] \\ & +\rho S_\beta[C_\alpha-\sqrt{3}S_\alpha]Z_c \end{aligned} \tag{6}$$

$$\begin{aligned} L_3^2 = {} & 1+\rho^2+X_c^2+Y_c^2+Z_c^2+X_c+\sqrt{3}\,Y_c \\ & -\rho[C_\alpha^2C_\beta+S_\alpha^2+\sqrt{3}\,C_\alpha S_\alpha(C_\beta-1)]\left[X_c+\frac{1}{2}\right] \\ & -\rho[S_\alpha C_\alpha(C_\beta-1)+\sqrt{3}(S_\alpha^2C_\beta+C_\alpha^2)]\left[Y_c+\frac{\sqrt{3}}{2}\right] \\ & +\rho S_\beta[C_\alpha+\sqrt{3}S_\alpha]Z_c \end{aligned} \tag{7}$$

where $S_\alpha = \sin\alpha$, $C_\alpha = \cos\alpha$, $S_\beta = \sin\beta$, $Z_c = z_c/R$, and $L_i = l_i/R$, $i = 1, 2, 3$. For a prescribed position and orientation of the moving platform, the dependent variables are defined by (2)–(4). Equations (5)–(7) are the inverse kinematic equations which define the actuating lengths of the links.

B. Forward Kinematics

The forward kinematic can be obtained by noting that the in-parallel actuated manipulator is essentially a rigid structure for a given set of link lengths. As the distance between the adjacent ball joints is $\sqrt{3}r$, the implicit relationship between the link lengths L_1, L_2, and L_3 and the angles θ_1, θ_2, and θ_3 are

$$L_1^2+L_2^2+3-3\rho^2+L_1L_2\cos\theta_1\cos\theta_2 - 2L_1L_2\sin\theta_1\sin\theta_2-3L_1\cos\theta_1-3L_2\cos\theta_2=0 \tag{8}$$

$$L_2^2+L_3^2+3-3\rho^2+L_2L_3\cos\theta_2\cos\theta_3 - 2L_2L_3\sin\theta_2\sin\theta_3-3L_2\cos\theta_2-3L_3\cos\theta_3=0 \tag{9}$$

$$L_3^2+L_1^2+3-3\rho^2+L_3L_1\cos\theta_3\cos\theta_1 - 2L_3L_1\sin\theta_3\sin\theta_1-3L_3\cos\theta_3-3L_1\cos\theta_1=0 \tag{10}$$

where θ_i with $i = 1, 2, 3$ is defined to be the angle between the ith link and the base platform as shown in Fig. 1.

Local rigidity, however, does not imply uniqueness; multiple solutions of θ_1, θ_2, and θ_3 corresponding to a given set of link lengths are possible. The further mathematical constraint which is necessary to ensure uniqueness is

$$0° < \theta_i < 180°.$$

In other words, the Cartesian position z_c of the moving platform must be positive or the moving platform must always be on one side of the base platform. This criterion is a physical constraint on the hardware,not just mathematical artifacts. The physical constraints are imposed by the range of pin joints and the ball joints, which were discussed in [15].

For a given set of link lengths, the corresponding angles θ_i can be computed numerically from (8)–(10), which are implicit relationships between L_i and θ_i, where $i = 1, 2, 3$.

Cartesian Position of Moving Platform: Since the ball joints are placed at the vertices of an equilateral triangle, the Cartesian position or the origin of the xyz frame can be determined as

$$X_c = \frac{1}{3}\sum_{i=1}^{3}\frac{x_{bi}}{R}$$

$$Y_c = \frac{1}{3}\sum_{i=1}^{3}\frac{y_{bi}}{R}$$

$$Z_c = \frac{1}{3}\sum_{i=1}^{3}\frac{z_{bi}}{R} \tag{11}$$

where the ball-joint coordinates with respect to the base frame are

$$X_{b1} = 1 - L_1 \cos\theta_1$$

$$Y_{b1} = 0$$

$$Z_{b1} = L_1 \sin\theta_1 \tag{12}$$

$$X_{b2} = -\frac{1}{2}(1 - L_2\cos\theta_2)$$

$$Y_{b2} = +\frac{\sqrt{3}}{2}(1 - L_2\cos\theta_2)$$

$$Z_{b2} = L_2 \sin\theta_2 \tag{13}$$

$$X_{b3} = -\frac{1}{2}(1 - L_3\cos\theta_3)$$

$$Y_{b3} = -\frac{\sqrt{3}}{2}(1 - L_3\cos\theta_3)$$

$$Z_{b3} = L_3 \sin\theta_3. \tag{14}$$

Orientation of Moving Platform: With the Cartesian position of the ball joints defined in (12)–(14), the orientation of the moving platform can be determined by noting that the Cartesian position of the ball joints can also be expressed as

$$X_{b1} = \rho n_1 + X_c$$

$$Y_{b1} = \rho n_2 + Y_c$$

$$Z_{b1} = \rho n_3 + Z_c \tag{15}$$

$$X_{b2} = -\frac{1}{2}\rho n_1 + \frac{\sqrt{3}}{2}\rho o_1 + X_c$$

$$Y_{b2} = -\frac{1}{2}\rho n_2 + \frac{\sqrt{3}}{2}\rho o_2 + Y_c$$

$$Z_{b2} = -\frac{1}{2}\rho n_3 + \frac{\sqrt{3}}{2}\rho o_3 + Z_c \tag{16}$$

$$X_{b3} = -\frac{1}{2}\rho n_1 - \frac{\sqrt{3}}{2}\rho o_1 + X_c$$

$$Y_{b3} = -\frac{1}{2}\rho n_2 - \frac{\sqrt{3}}{2}\rho o_2 + Y_c$$

$$Z_{b3} = -\frac{1}{2}\rho n_3 - \frac{\sqrt{3}}{2}\rho o_3 + Z_c. \tag{17}$$

To determine the orientation of the moving platform, the directional cosines, which are denoted as the components of the vectors $\boldsymbol{n}$, $\boldsymbol{o}$, and $\boldsymbol{a}$ in the homogeneous transformation $[T]$, are expressed in terms of θ_i. By equating (12) and (15), the components of the normal vector $\boldsymbol{n}$ can be determined as

$$n_1 = \frac{1 - L_1\cos\theta_1 - X_c}{\rho}$$

$$n_2 = -\frac{Y_c}{\rho}$$

$$n_3 = \frac{L_1\sin\theta_1 - Z_c}{\rho}. \tag{18}$$

Similarly, equating (13) and (16), the orientation vector $\boldsymbol{o}$ is

$$o_1 = n_2$$

$$o_2 = \frac{\sqrt{3} - \sqrt{3}L_2\cos\theta_2 - 3Y_c}{\sqrt{3}\rho}$$

$$o_3 = \frac{2L_2\sin\theta_2 + L_1\sin\theta_1 - 3Z_c}{\sqrt{3}\rho}. \tag{19}$$

As the unit vectors $\boldsymbol{n}$, $\boldsymbol{o}$, and $\boldsymbol{a}$ form an orthogonal set, the components of the approach vector $\boldsymbol{a}$ can be determined as

$$a_1 = n_2 o_3 - o_2 n_3$$

$$a_2 = -n_1 o_3 + o_1 n_3$$

$$a_3 = n_1 o_2 - n_2 o_1. \tag{20}$$

Hence, for a given set of link length, (8)–(10) are computed numerically for the angles θ_i. The Cartesian position is then computed from (11) and the orientation is obtained by computing the directional cosines of the axes x, y, and z with respect to the base frame XYZ from (18)–(20).

III. Formulation of Dynamic Equations

The equations of motion which describe the actuating forces required to cause motion are derived using Lagrangian approach. In the following dynamic analysis, the dynamics of the gripper are not included and the moving platform is assumed to be a circular plate. The mass of the moving platform is therefore assumed to have the center of gravity at the origin of the xyz frame. Since the actuating forces acting on the links F_1, F_2, and F_3, are to be found, the normalized link lengths L_1, L_2, and L_3, are chosen to be the independent generalized coordinates and θ_1, θ_2, and θ_3 are the dependent generalized coordinates. The three constraint equations relating L_i and θ_i are given in (8)–(10).

The kinetic co-energy of the mechanism can be written as

$$T=\frac{1}{2}M(\dot{x}_c^2+\dot{y}_c^2+\dot{z}_c^2)+\frac{1}{2}(I_{xx}\omega_x^2+I_{yy}\omega_y^2+I_{zz}\omega_z^2)+\frac{1}{2}m\sum_{i=1}^{3}d_i^2\dot{\theta}_i^2 \tag{21}$$

where

M	mass of the moving platform,
m	mass of the link,
d_i	distance between the pin joint and the centroid of each link,
ω_x, ω_y, ω_z	angular velocity of the body axes of the moving platform with respect to a moving frame parallel to the XYZ frame,
I_{xx}, I_{yy}, I_{zz}	moment of inertia of the moving platform about x, y, and z, respectively.

Due to the symmetry of the circular platform, I_{xy}, I_{yz}, and I_{zx} are identically equal to zero. The moments of inertia are

$$I_{xx}=I_{yy}=\frac{1}{2}I_{zz}=\frac{1}{4}Mr^2.$$

The potential energy of the mechanism is given by

$$P=Mgz_c+mg\sum_{i=1}^{3}d_i\sin\theta_i. \tag{22}$$

The Lagrangian equations of motion become

$$\frac{d}{dt}\left(\frac{\partial\mathcal{L}}{\partial\dot{q}_i}\right)-\frac{\partial\mathcal{L}}{\partial q_i}+\sum_{k=1}^{3}\lambda_k\frac{\partial f_k}{\partial q_i}=Q_i, \qquad i=1,\cdots,6 \tag{23}$$

where

$$\mathcal{L}=T-P$$

$$q_i=\begin{cases} l_i, & i=1,2,3 \\ \theta_i, & i=4,5,6 \end{cases}$$

$$Q_i=\begin{cases} F_i, & i=1,2,3 \\ T_{i-3}, & i=4,5,6 \end{cases}$$

and where F_i is the actuating force along the ith link and T_{i-3}, $i=4$, 5, 6 are frictional torques of the ith link in the θ_i direction. In the following discussion, the frictional torques are assumed to be zero. The constraint equations are

$$f_k(L_1, L_2, L_3, \theta_1, \theta_2, \theta_3)=0 \tag{24}$$

where $k=1, 2, 3$. Note that $f_k(L_i, \theta_i, i=1, 2, 3)$ are the constraint equations (8)–(10), respectively.

IV. Determination of the Velocity Components

As the link lengths and the angles L_i and θ_i have been chosen as generalized coordinates, the Cartesian velocity and the angular velocity must be expressed as a function of L_i and θ_i and their derivatives with respect to time. The Cartesian position is a function of L_i and θ_i as shown in (11). The Cartesian velocity can be obtained by directly differentiating (11) with respect to time such that

$$\boldsymbol{V}_c=\sum_{i=1}^{3}\frac{\partial\boldsymbol{X}_c}{\partial L_i}\frac{dL_i}{dt}+\sum_{i=1}^{3}\frac{\partial\boldsymbol{X}_c}{\partial\theta_i}\frac{d\theta_i}{dt} \tag{25}$$

where $\boldsymbol{X}_c(X_c, Y_c, Z_c)$ and $\boldsymbol{V}_c(X_c, Y_c, Z_c)$ are position and velocity vectors, respectively. The angular velocity, $\boldsymbol{\omega}(\omega_x, \omega_y, \omega_z)$, in terms of the generalized coordinates can be determined by noting that the velocity of the ball joint may be written as

$$\boldsymbol{V}_{bi}=\boldsymbol{V}_c+\boldsymbol{\omega}\times\boldsymbol{r}_i \tag{26}$$

where $\boldsymbol{r}_i$ is the line vector directed from the ith ball joint to the center of the moving platform. From the geometry, $\boldsymbol{r}_i$ can be written as

$$\boldsymbol{r}_1=\rho\boldsymbol{i}$$

$$\boldsymbol{r}_2=\left(-\frac{1}{2}\boldsymbol{i}+\frac{\sqrt{3}}{2}\boldsymbol{j}\right)\rho$$

$$\boldsymbol{r}_3=\left(-\frac{1}{2}\boldsymbol{i}-\frac{\sqrt{3}}{2}\boldsymbol{j}\right)\rho. \tag{27}$$

The velocity of the ball joints with respect to the base frame is

$$\boldsymbol{V}_{bi}=\dot{L}_i\boldsymbol{\phi}_{li}+\dot{\theta}_i\boldsymbol{\phi}_{zi}\times L_i\boldsymbol{\phi}_{li} \tag{28}$$

where $\boldsymbol{\phi}_{li}$ and $\boldsymbol{\phi}_{zi}$ are the unit vectors along the ith link length and along the axis of the ith pin joint, respectively. In terms of the unit vectors of the base frame, the vectors are

$$\boldsymbol{\phi}_{li}=-\cos\theta_1\boldsymbol{I}+\sin\theta_1\boldsymbol{K}$$

$$\boldsymbol{\phi}_{l2}=\frac{1}{2}\cos\theta_2\boldsymbol{I}-\frac{\sqrt{3}}{2}\cos\theta_2\boldsymbol{J}+\sin\theta_2\boldsymbol{K}$$

$$\boldsymbol{\phi}_{l3}=\frac{1}{2}\cos\theta_3\boldsymbol{I}+\frac{\sqrt{3}}{2}\cos\theta_3\boldsymbol{J}+\sin\theta_3\boldsymbol{K} \tag{29}$$

and

$$\boldsymbol{\phi}_{z1}=\boldsymbol{J}$$

$$\boldsymbol{\phi}_{z2}=-\frac{\sqrt{3}}{2}\boldsymbol{I}-\frac{1}{2}\boldsymbol{J}$$

$$\boldsymbol{\phi}_{z3}=\frac{\sqrt{3}}{2}\boldsymbol{I}-\frac{1}{2}\boldsymbol{J}. \tag{30}$$

By equating (26) and (28) for the ith ball joint and noting that the unit vector (i, j, k) may be transformed to (I, J, K) through the homogeneous transformation $[T]$, the angular velocities $\boldsymbol{\omega}(\omega_x, \omega_y, \omega_z)$ can be derived by equating the appropriate vector components as

$$\begin{aligned}\omega_x=\frac{2}{\sqrt{3}}\frac{1}{\rho}\Bigg[&a_1\left(\frac{1}{2}\dot{L}_2\cos\theta_2-\frac{1}{2}L_2\sin\theta_2\cdot\dot{\theta}_2-\dot{X}_c\right)\\ &+a_2\left(-\frac{\sqrt{3}}{2}-\dot{L}_2\cos\theta_2+\frac{\sqrt{3}}{2}L_2\sin\theta_2\cdot\dot{\theta}_c-\dot{Y}\right)\\ &+a_3(\dot{L}_2\sin\theta_2+L_2\cos\theta_2\cdot\dot{\theta}_2-\dot{Z}_c)-\frac{\rho}{2}\omega_y\Bigg]\end{aligned} \tag{31}$$

$$\begin{aligned}\omega_y=-\frac{1}{\rho}[&a_1(-\dot{L}_1\cos\theta_1+L_1\sin\theta_1\cdot\dot{\theta}_1-\dot{X}_c)-a_2\dot{Y}\\ &+a_3(\dot{L}_1\sin\theta_1+L_1\cos\theta_1\cdot\dot{\theta}_1-\dot{Z}_c)]\end{aligned} \tag{32}$$

$$\omega_z = -\frac{2}{\rho}\left[o_1\left(\frac{1}{2}\dot{L}_2\cos\theta_2 - \frac{1}{2}L_2\sin\theta_2\dot{\theta}_2 - \dot{X}_c\right)\right.$$
$$+ o_2\left(-\frac{\sqrt{3}}{2}\dot{L}_2\cos\theta_2 + \frac{\sqrt{3}}{2}L_2\sin\theta_2\dot{\theta}_2 - \dot{Y}_c\right)$$
$$\left. + o_3(\dot{L}_2\sin\theta_2 + L_2\cos\theta_2\cdot\dot{\theta}_2 - \dot{Z}_c)\right]. \tag{33}$$

V. Determination of Actuating Forces

In many real-time applications of on-line control of the manipulator, the Cartesian position/orientation and the respective velocity and acceleration of the moving platform are known or predetermined. It is of interest to determine the forces required to actuate the links so that the manipulator follows a predetermined trajectory.

The kinetic coenergy T, the potential energy P, and the constraint equations f_k, are functions of L_i, θ_i, and their time derivatives. From (23), the force required to actuate the ith link is

$$F_i = \frac{d}{dt}\left(\frac{\partial T}{\partial \dot{l}_i}\right) - \frac{\partial T}{\partial l_i} + \frac{\partial P}{\partial l_i} + \sum_{k=1}^{3}\lambda_k\frac{\partial f_k}{\partial l_i} \tag{34}$$

where $i = 1, \cdots, 6$ and the three unknown Lagrangian multipliers λ_j can be solved from the three simultaneous equations, i.e., (23) with $i = 4, 5, 6$, using Cramer's rule. The actuating force along the ith link can be computed by directly differentiating T, P, and f_k with respect to l_i and its derivatives.

VI. An Example of Dynamic Simulation

An example of tracing a helical path is simulated to illustrate the above dynamic analysis. Although it is more practical to assume the manipulator has two orientation freedoms in addition to a third freedom in the z direction, the example illustrates that the Cartesian coordinates of the center point of the moving platform may be controlled at the sacrifice of orientation freedoms. The example is simulated with the following assumptions: 1) The pin and ball joints are assumed to be frictionless. 2) The position variation of the center of gravity of each link is negligible, i.e., d_i is constant.

The helical path to be traced has a radius r^* and a pitch h. The helical path with respect to the base frame can be described by the following equation:

$$x = r^*\cos\phi$$
$$y = r^*\sin\phi$$
$$z = z_i + \frac{h}{T^*}t \tag{35}$$

where T^* is the time required to travel one pitch, t is the time variable, and z_i is any particular starting z. As the center point of the moving platform is to follow the helical path, (3) and (4) are equated to the x and y components of (35) yielding

$$2\alpha + \phi = n\pi, \qquad n = 0, \pm 1, \pm 2 \cdots \tag{36}$$
$$\cos\beta = 2\frac{r^*}{r} + 1. \tag{37}$$

Differentiating (36) with respect to time

$$\dot{\alpha} = -\frac{1}{2}\dot{\phi} \tag{38}$$

the rate of change of ϕ with respect to time is linearly proportional to α and β remains constant with respect to time for a constant r^*. The trajectory can be planned based on ϕ noting that the total time required for one helical path must be equal to T^*. The parameters of the trajectory are summarized in Table I and the parameters used for simulation are listed in Table II.

TABLE I
Trajectory of the Simulation

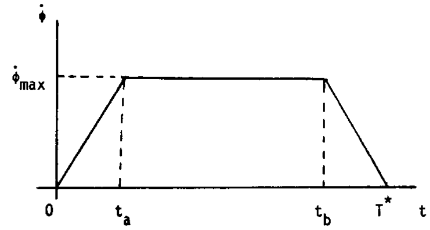

$$\alpha = -\frac{1}{2}\int\dot{\phi}\,dt + \frac{\pi}{2}$$
$$\dot{\alpha} = -\frac{1}{2}\dot{\phi}$$
$$\ddot{\alpha} = -\frac{1}{2}\ddot{\phi}$$
$$\beta = \cos^{-1}\left[2\left(\frac{r^*}{r}\right) + 1\right]$$
$$\dot{\beta} = 0$$
$$\ddot{\beta} = 0$$
$$Z_c = Z_i + \frac{h}{T^*}t$$
$$\dot{Z}_c = \frac{h}{T^*}$$
$$\ddot{Z}_c = 0$$

TABLE II
Parameters for Simulation

Manipulator Parameters		
	R	= 0.2286 m
	ρ	= 0.5
	D_m	= 0.5334 m*
	M	= 0.18 kg
	m/M	= 0.5
	d_i	= 0.1524 m
Helix Parameters		
	r^*	= 0.266 mm
	h	= 0.03048 m
	z_i	= 0.3048 m
Trajectory Parameters		
	T^*	= 10 s
	t_a	= 1 s
	t_b	= 9 s
	ϕ_{max}	= 2/9 π

* D_m is the distance between the center of the moving platform and the intersection between the axis of the ball-joint socket and the normal of the moving platform through the center [15].

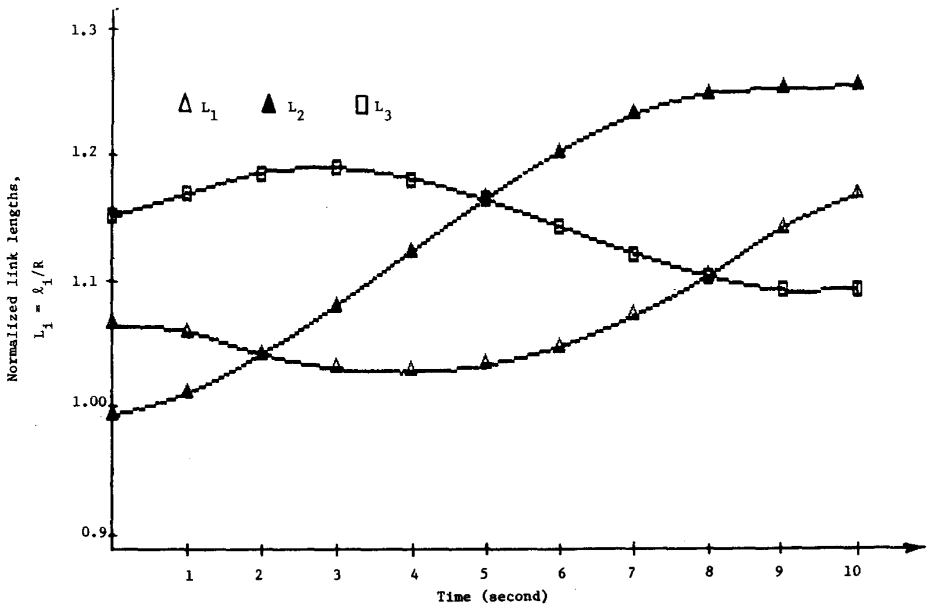

Fig. 2. Actuating lengths as a function of time.

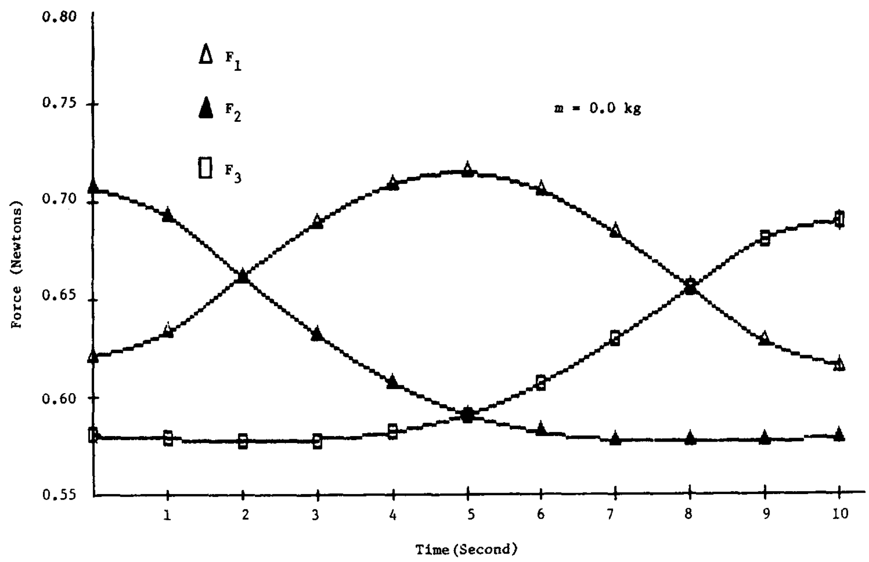

Fig. 3. Computed actuating forces for $m = 0.0$.

The corresponding actuating lengths are computed from the inverse kinematics as shown in Fig. 2 and the angles θ_i are determined from the following relationship:

$$\sin \theta_i = \frac{Z_{bi}}{L_i} \tag{39}$$

where Z_{bi} is given in (15)–(17).

The actuating forces for the specified trajectory are computed for the following two cases: 1) The mass of eah link is assumed to be very small compared with the mass of the moving platform. This is particularly true for tendon actuated manipulator and is a good assumption for hydraulic actuated manipulator with high payload at the gripper. 2) The mass of the link is not negligible but $m/M = 0.5$. The objective is to determine the effect of the mass dynamics of the links. The simulation outputs for $m = 0.0$ and $m = 0.09$ kg are shown in Figs. 3 and 4, respectively. The result has shown that the forces required have been increased by approximately 20 percent due to the mass dynamics of the links.

VII. Conclusion

The dynamic analysis of a 3-DOF in-parallel actuated manipulator, which is characterized by its excellent rigidity, high strength-to-moving-weight ratio, and relatively simple inverse kinematics, has been formulated using Lagrangian approach. The inverse dynamic model, which predicts the forces required to actuate the links so that the manipulator follows a predetermined trajectory, are derived in joint space. The actuating link lengths of the manipulator are chosen as generalized coordinates and the velocity components have been expressed in terms of the generalized coordinates.

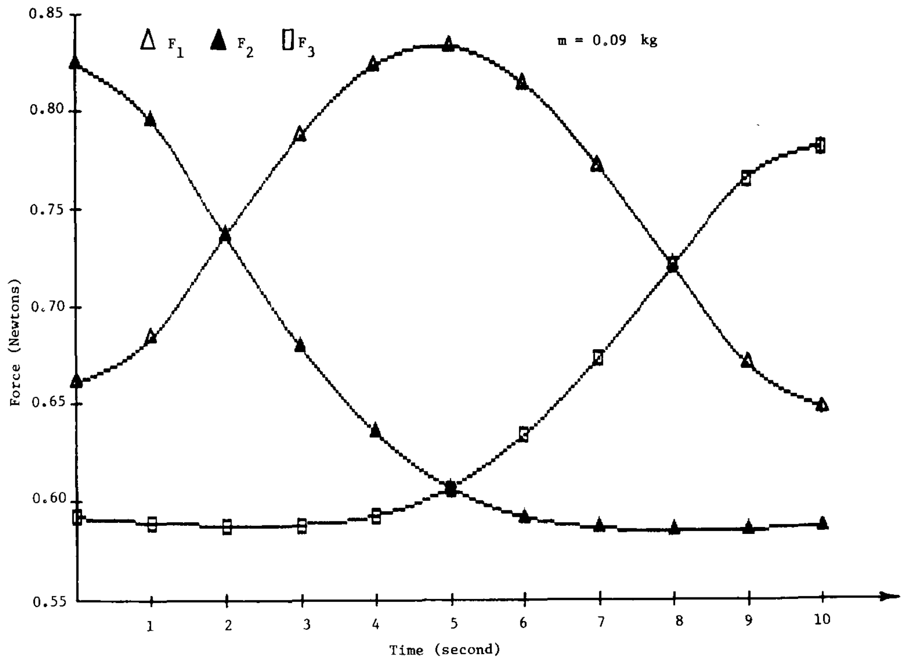

Fig. 4. Computing actuating force on $m/M = 0.5$.

In addition, a dynamic simulation program has been developed and a numerical example of tracing a helical path has been chosen to demonstrate the dynamic simulation. The result of the simulation illustrates the influence of the link dynamics on the actuating forces required. The dynamic model, which is essential for feedforward control of the manipulator, will serve as a basis for prototype design, control scheme development, prediction of inertia parameters. Future work will include prototype design and real-time simulation computer control scheme development and performance evaluation in an industrial environment.

Acknowledgment

The authors would like to thank Dr. W. Book, CIMS director, for establishing their contact with the CIMS program and for providing a stimulating research environment.

References

[1] D. Stewart, "A platform with six degrees of freedom," *Proc. Inst. Mech. Eng.*, vol. 180, pt. 1, no. 15, pp. 371–386, 1965/1966.

[2] W. M. Bennett, "A mechanical wrist for a robot arm," B.S. thesis, MIT, Cambridge, MA, 1968.

[3] K. H. Lim, "Control of a tendon arm," MIT, Cambridge, MA, MIT A. I. Memo 617, Feb. 1981.

[4] S. E. Landsberger, "Design and construction of a cable-controlled, parallel link manipulator," MIT, Cambridge, MA, S. M. thesis, Sept. 1984.

[5] H. McCallion and P. D. Truong, "The analysis of a six-degree-of-freedom work station for mechanized assembly," in *Proc. 5th World Congr. for the Theory of Machines and Mechanisms* (an ASME publ.), pp. 611–616, 1979.

[6] H. McCallion, G. R. Johnson, and D. T. Phan, "A compliant device for inserting a peg into a hole," *The Industrial Robot*, June 1979.

[7] D. C. H. Yang and T. W. Lee, "Feasibility study of a platform type of robotic manipulators from a kinematic viewpoint," *J. Mech. Transmiss. Automat. Des.*, vol. 106, pp. 191–198, June 1984.

[8] E. F. Fichter, "A Steward platform-based manipulator: General theory and practical construction," *Int. J. Robotics Res.*, vol. 5, no. 2, Summer 1986.

[9] K. H. Hunt, "Structural kinematics of in-parallel-actuated robot arms," *Trans. ASME, J. Mechanisms, Transmiss. Automat. Des.*, vol. 105, pp. 705–712, 1983.

[10] E. F. Fichter and E. D. McDowell, "A novel design for a robot arm," *Adv. Comput. Technol.* (an ASME Publ.) pp. 250–256, 1980.

[11] W. Q. DoDo and D. C. H. Yang, "Inverse dynamics of a platform type of manipulating structure," presented at the ASME Design Engineering Technical Conf., Columbus, OH, Oct. 5–8, 1986, publ. 86-DET-94.

[12] K. Sugimoto, "Kinematic and dynamic analysis of parallel manipulators by means of motor algebra," presented at the ASME Engineering Technical Conf., Columbus, OH, Oct. 5–8, 1986, publ. 86-DET-139.

[13] Z. Huang and H. B. Wang, "Modeling formulation of six-DOF multi-loop parallel manipulation: Part 2. Dynamic modeling and example," in *Proc. 4Th IFTONM Symp. on Linkage and CAD Design Methods*, paper 21, vol. 2-1 (Bucharest, Romania, July 4–9, 1985).

[14] Z. Huang and H. B. Wang, "Dynamic force analysis of six-DOF parallel multi-loop robot manipulators," presented at the ASME Engineering Technical Conf., Columbus, OH., Oct. 5–8, 1986, publ. 86-DET-168.

[15] K. M. Lee and D. Shah, "Kinematic analysis of a three degrees of freedom in-parallel actuated manipulator," in *Proc. 1987 IEEE Int. Conf. on Robotics and Automation* (Raleigh, NC). Also, this issue, pp. 354–360.

[16] K. M. Lee, A. Chao, and D. K. Shah, "A three degrees of freedom in-parallel actuated manipulator," in *Proc. Int. Conf. on Applied Control and Identification* (Los Angeles, CA, Dec. 10–12, 1986).

[17] G. Vachetsevanos, K. Devey, and K. M. Lee, "On the development of a novel intelligent roboric manipulator," in *Proc. 1986 IEEE Int. Conf. on System, Man-Machine and Cybernetics* (Atlanta, GA, Oct. 1986). Also, in *IEEE Contr. Syst. Mag.*, vol. 7, no. 3, June 1987.

[18] J. J. Craig, *Introduction to Robotics, Mechanics and Control.* Reading, MA: Addison-Wesley, 1985.